Electronic Supplementary Material (ESI) for Materials Advances.
This journal is © The Royal Society of Chemistry 2020

Supporting Information

Defect induced "Super mop" like behaviour of Eu^{3+}-doped hierarchical Bi_2SiO_5 nanoparticles for improved catalytic and adsorptive behaviour

Debashrita Sarkar, Sagar Ganguli, Athma E. Praveen and Venkataramanan Mahalingam*

Department of Chemical Sciences, Indian Institute of Science Education and Research Kolkata, India

Email: mvenkataramanan@yahoo.com

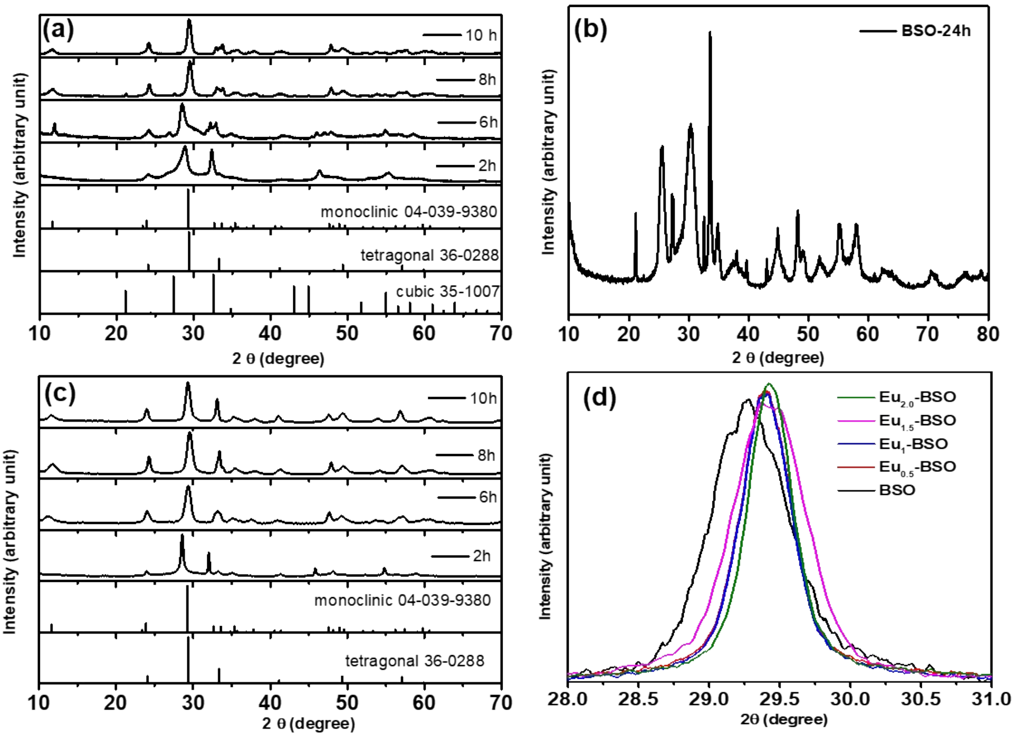

Fig. S1: (a) PXRD pattern for time dependent formation of $Eu_{1.5}$-BSO nanoparticles (b) PXRD pattern of BSO nanoparticles formed after 24h (c) PXRD pattern for time dependent formation of BSO nanoparticles and (d) Normalised intensity of (100) plane depicting shift in 2θ due to Eu^{3+} doping.

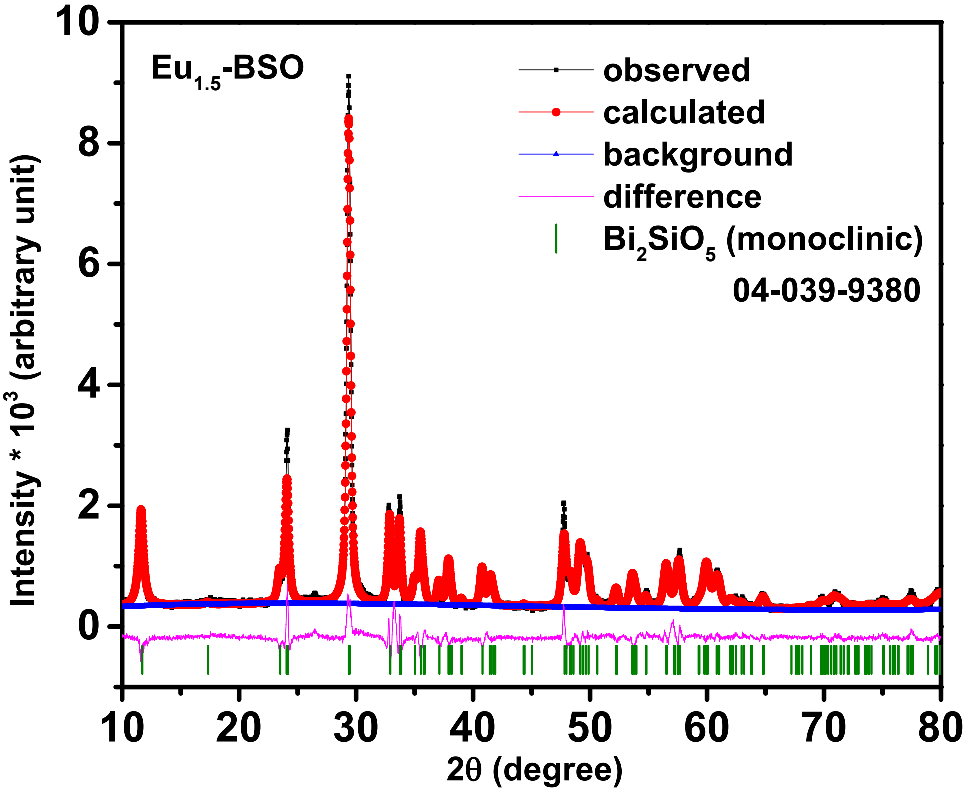

Fig. S2: Rietveld refinement of $Eu_{1.5}$-BSO nanoparticles.

Table S1: Crystallographic data of $(Bi_{0.985}Eu_{0.15})_2SiO_5$ determined using Reitveld refinement.

Formula	$(Bi_{0.985}Eu_{0.15})_2SiO_5$				
Crystal System	Monoclinic				
Space Group	Cc				
Cell parameters	a=15.11368 Å ,b= 5.42673 Å ,c= 5.29606 Å α= γ= 90 ° β= 90.224°				
Cell Volume	434.368 $Å^3$				
Density	7.981				
R_{wp}	10.185%				
GOF	2.4				
Atom	**Wyckoff position**	**Occupancy**	**Atomic coordinates**		
			x	**y**	**z**
Bi1	4a	0.9850	0.1696	0.2166	0.2609
Bi2	4a	1	0.8399	0.2195	0.274
Si	4a	1	0.5057	0.172	0.2459
O1	4a	1	0.499	0.0166	0.5112
O2	4a	1	0.5858	0.3309	0.2247
O3	4a	1	0.4039	0.3233	0.2268
O4	4a	0.795	0.2497	0.4942	0.4949
O5	4a	1	0.2563	0.2563	0.2563
Eu	4a	0.015	0.1696	0.2166	0.2609

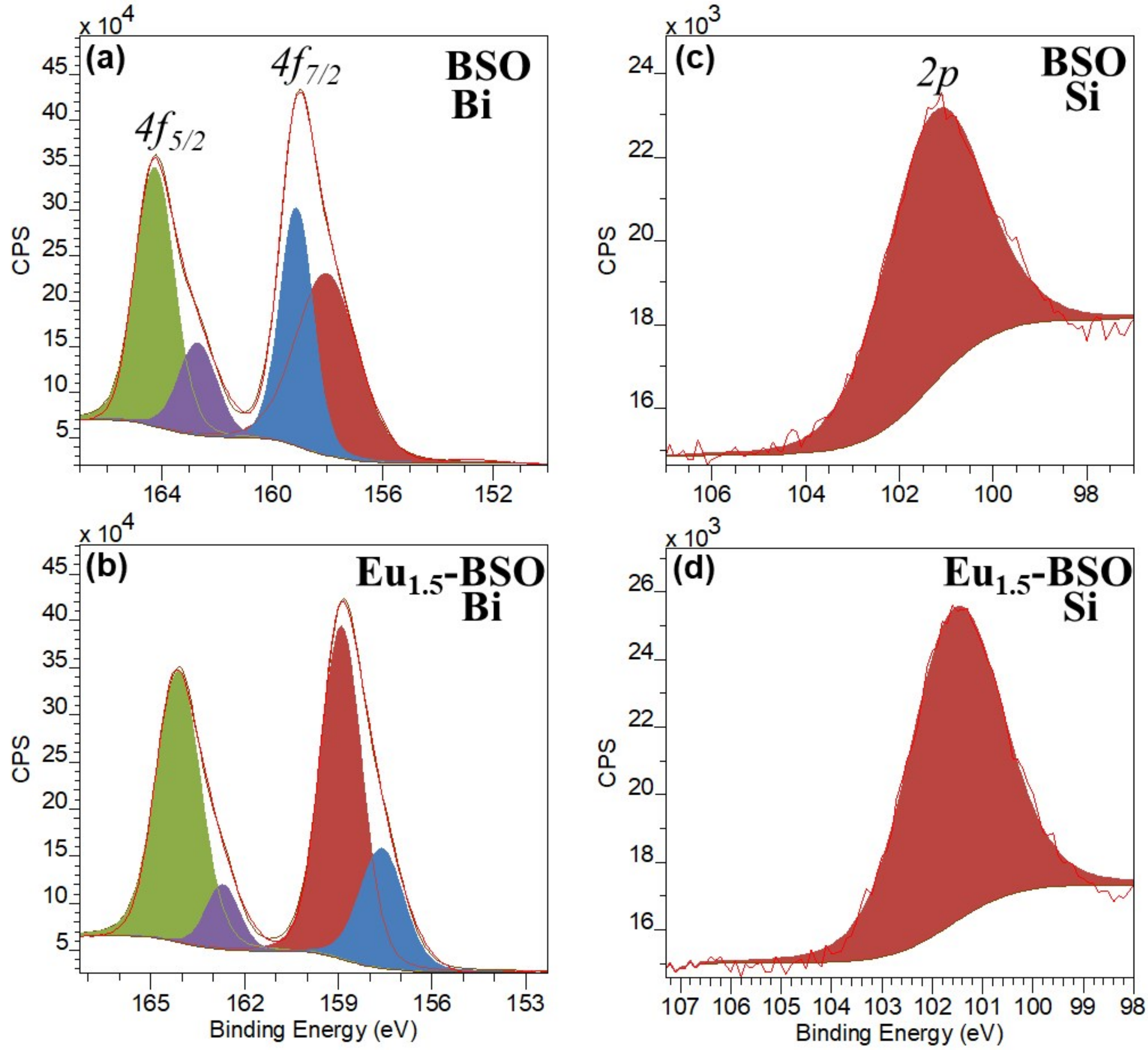

Fig. S3: XPS spectra of (a) Bi 4f for BSO, (b) Bi 4f for $Eu_{1.5}$-BSO, (c) Si 2p for BSO, and (d) Si 2p for $Eu_{1.5}$-BSO nanoparticles.

Table S2: Bond vibration of the different bonds obtained using Fourier Transformed Infrared spectroscopy.

	O-H (cm^{-1})	Si-O-Si Symmetric (cm^{-1})	Si-O-Si Asymmetric (cm^{-1})	SiO_4 Distorted (cm^{-1})	Si-O-Bi (cm^{-1})	Bi-O-Bi (cm^{-1})
BSO	3394	1380	1047	952	897,857	611
$Eu_{0.5}$ -BSO	3429	1385	1044	950	858	574
$Eu_{1.0}$ -BSO	3452	1424	1048	946	859	575
$Eu_{1.5}$ -BSO	3429	1473	1048	946	860	574
$Eu_{2.0}$ -BSO	3420	1454	1046	946	858	575

Table S3: ICP- Analysis of $Eu_{1.5}$-BSO nanoparticles

Sample Information	Bismuth (Atomic Mass=208.9804)			Europium (Atomic Mass=151.964)		
	ppm	mg/L	mmol/L	ppm	mg/L	mmol/L
Eu-BSO	46.404	46.404	0.222	0.491	0.491	0.003

Table S4: Elemental composition obtained using EDS for BSO and Eu-BSO nanoparticles

Sample	O	Si	Eu	Bi
BSO	68.9	9.33		21.69
$Eu_{0.5}$ -BSO	74.13	7.82	0.11	17.42
$Eu_{1.0}$ -BSO	76.7	7.14	0.21	15.95
$Eu_{1.5}$ -BSO	71.91	8.82	0.33	18.94
$Eu_{2.0}$ -BSO	73.20	7.93	0.34	18.52

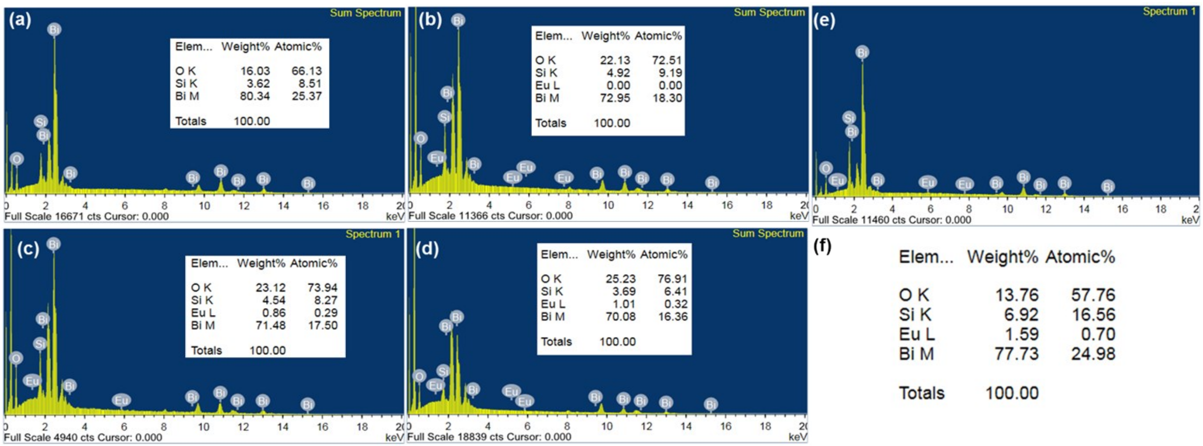

Fig. S4: EDS spectra for (a) BSO (b) $Eu_{0.5}$-BSO (c) Eu_1-BSO (d) $Eu_{1.5}$-BSO (inset shows the elemental composition) (e) Eu_2-BSO (f) elemental composition of Eu_2-BSO nanoparticles.

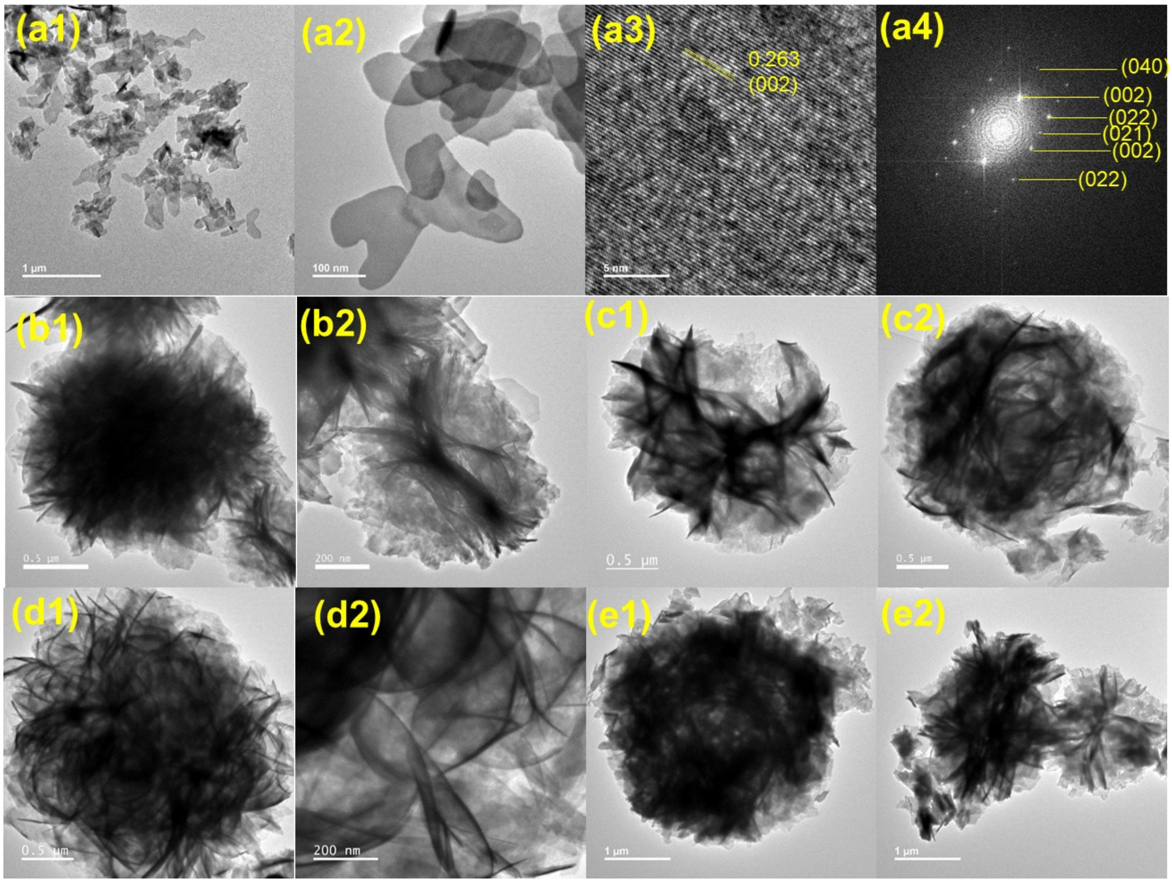

Fig. S5: TEM image of (a1-a2) BSO (a3) HRTEM image depicting interplaner distance corresponding to (002) plane (a4) FFT image depicting various planes for BSO (b1-b2) $Eu_{0.5}$-BSO nanoparticles (c1-c2) Eu_1-BSO nanoparticles (d1-d2) $Eu_{1.5}$-BSO nanoparticles (e1-e2) Eu_2-BSO nanoparticles.

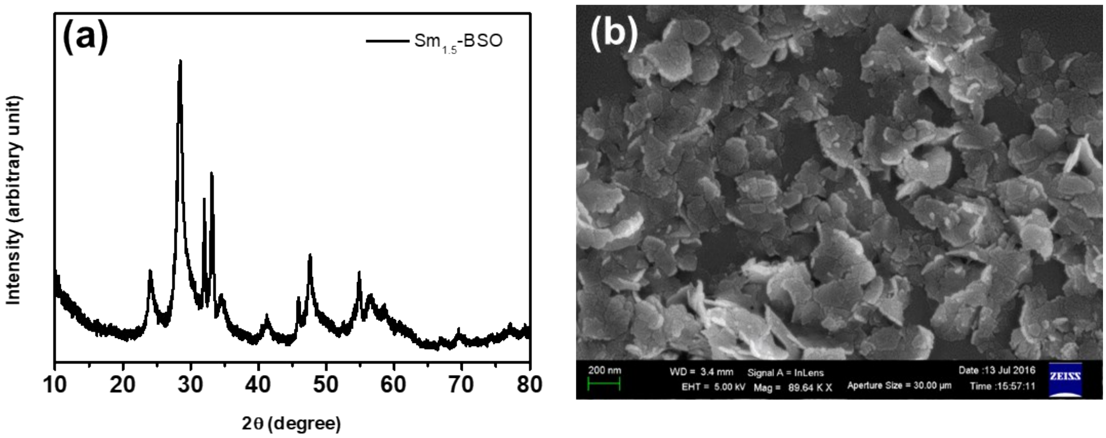

Fig. S6: (a) PXRD pattern of $Sm_{1.5}$-BSO nanoparticles depicting monoclinic phase (b) FESEM image of $Sm_{1.5}$-BSO nanoparticles.

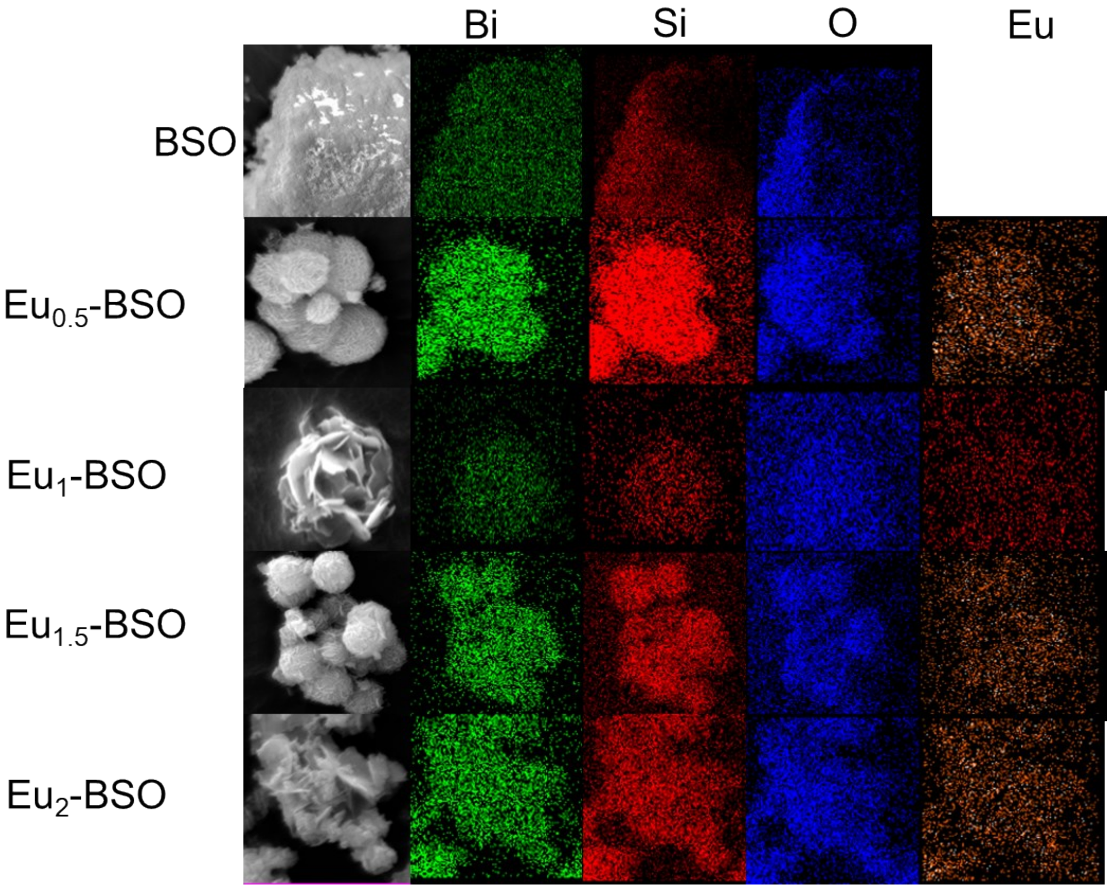

Fig. S7: Elemental mapping of BSO nanoparticles and Eu-BSO nanoparticles depicting the presence of Bi, Si, O, and Eu.

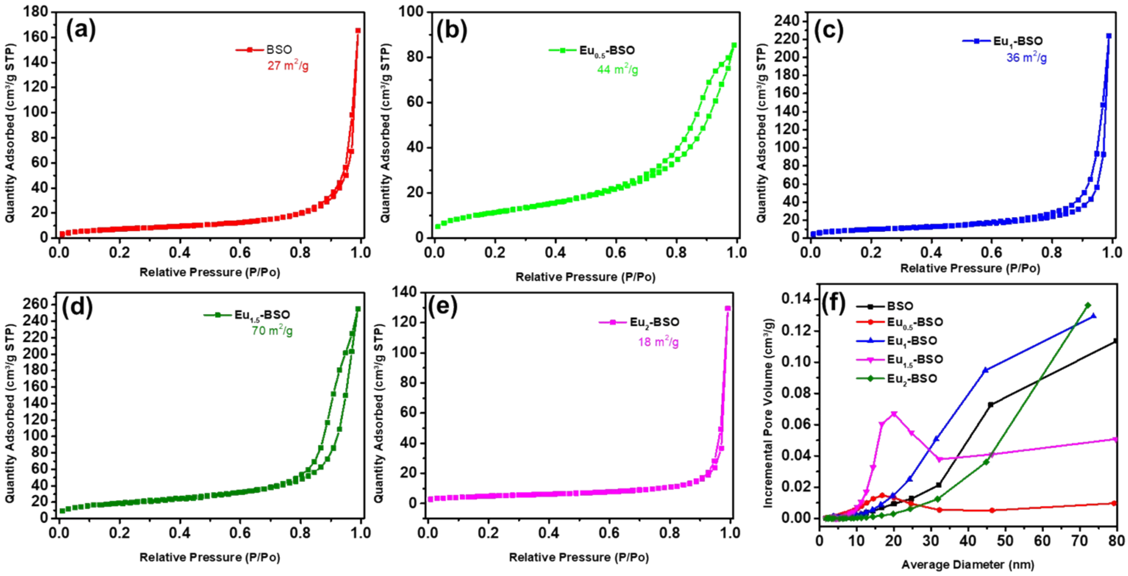

Fig. S8 : Nitrogen adsorption desorption isotherm of (a) BSO (b) $Eu_{0.5}$-BSO (c) $Eu_{1.0}$-BSO (d) $Eu_{1.5}$-BSO (e) $Eu_{2.0}$-BSO (f) BJH pore size distribution of BSO and Eu-BSO nanoparticles.

Table S5: Comparison of BET surface area, pore volume and pore size distribution of BSO and Eu-BSO nanoparticles.

Material information	BET Surface area (m^2/g)	Pore volume (cm^3/g)	Average pore diametre (nm)
BSO	27.1010 ± 0.0726	0.077821	2.22743
$Eu_{0.5}$ -BSO	43.6855 ± 0.1466	0.105733	16.81833
$Eu_{1.0}$ -BSO	35.6200 ± 0.1521	0.087918	3.62949
$Eu_{1.5}$ -BSO	70.1923 ± 0.2736	0.234135	20.0214
$Eu_{2.0}$ -BSO	17.5451 ± 0.0768	0.036943	20.0214

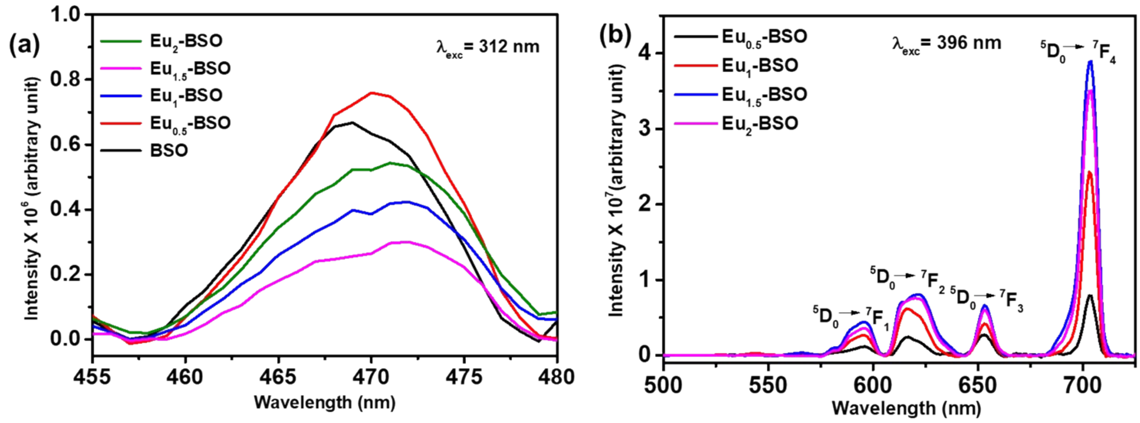

Fig. S9: (a) Photoluminescence of various Eu-BSO nanoparticles upon 312 nm excitation and (b) Photoluminescence of Eu^{3+} incorporated in various Eu-BSO nanoparticles upon 396 nm excitation.

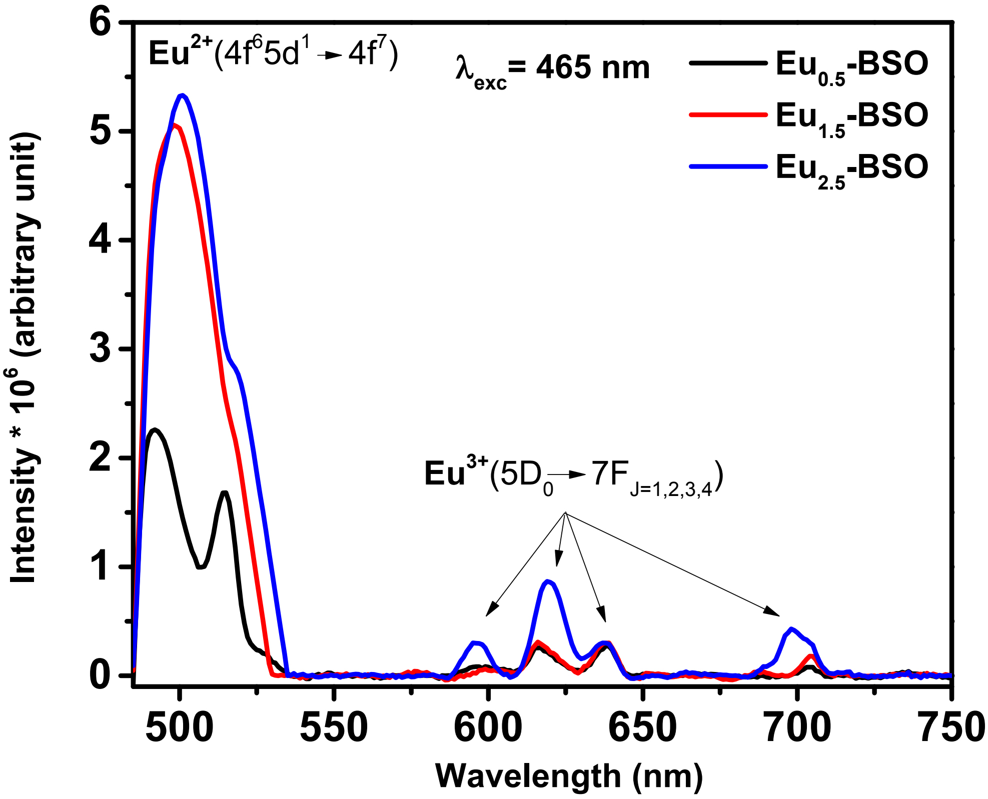

Fig. S10: Photoluminescence of various Eu-BSO nanoparticles upon 465 nm excitation.

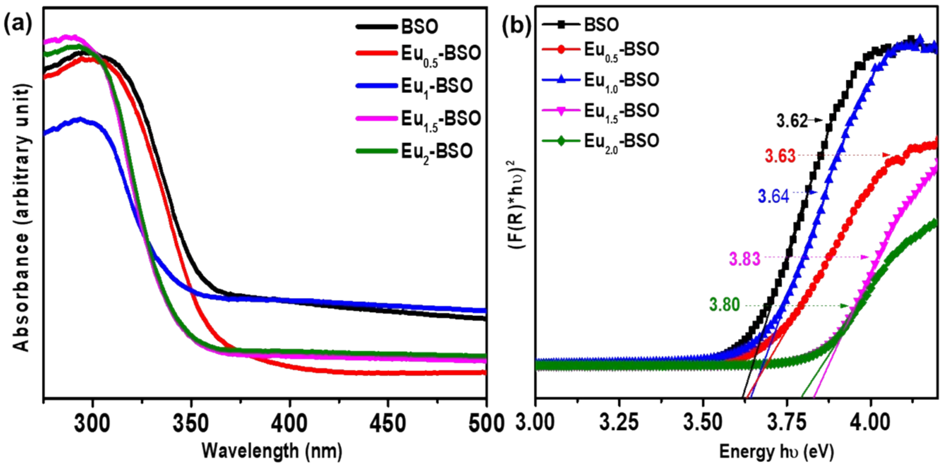

Fig. S11: (a) Absorption spectra of BSO nanoparticle and Eu-doped BSO nanoparticles (b) Kubelka-Munk plot for BSO and Eu-BSO nanoparticles.

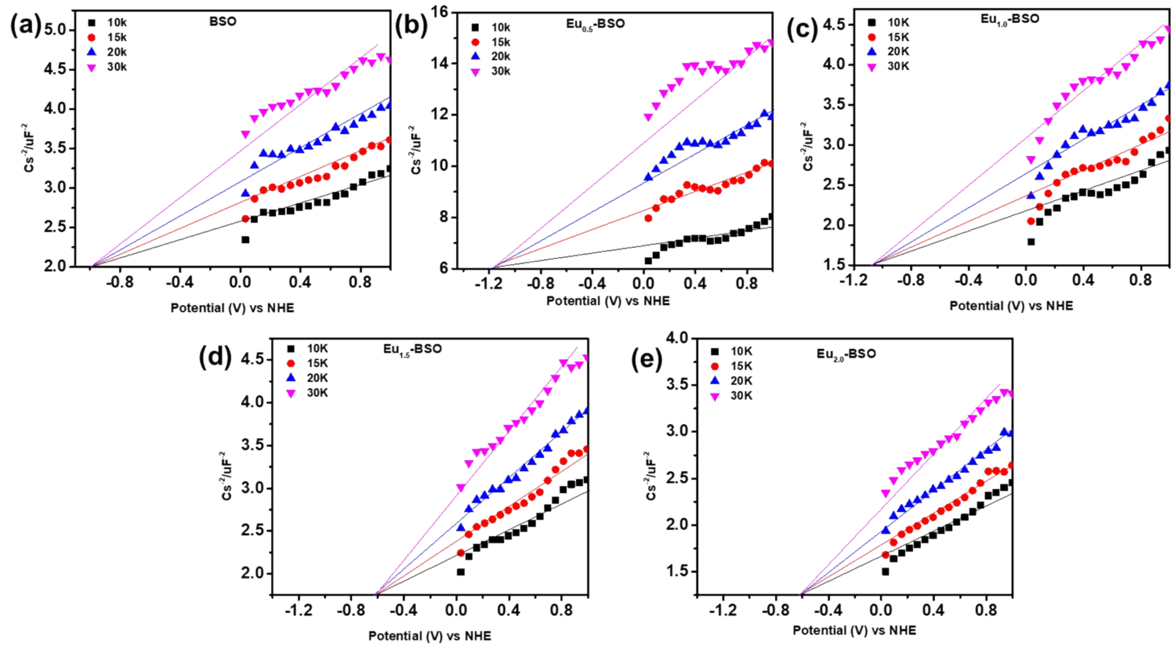

Fig. S12: Mott Schottky plot of (a) BSO (b) $Eu_{0.5}$-BSO (c) Eu_1-BSO (d) $Eu_{1.5}$-BSO (e) Eu_2-BSO.

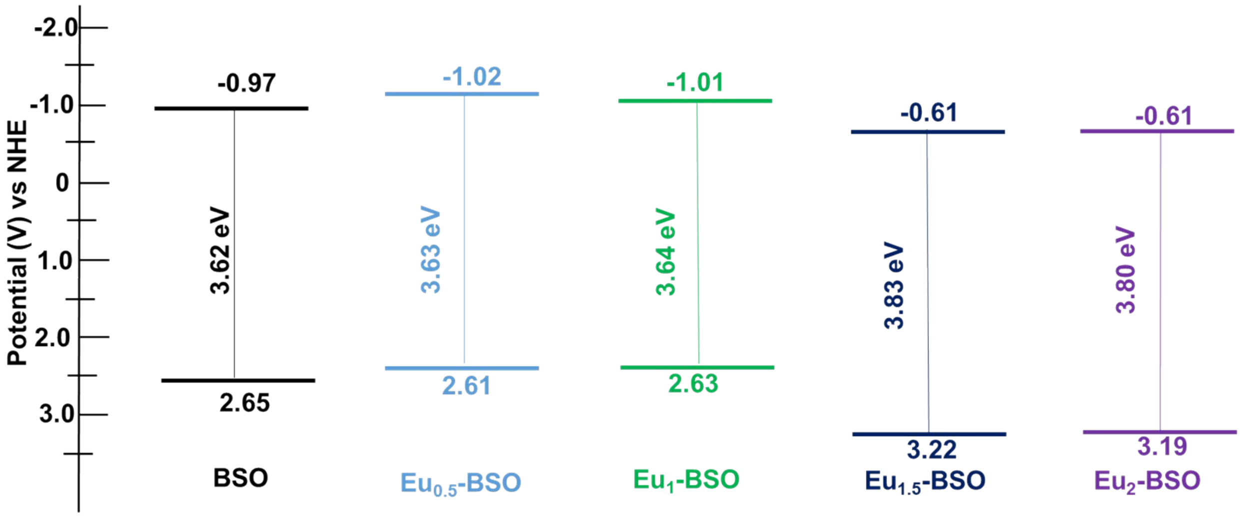

Fig. S13: Band edge potential of different Eu-BSO nanoparticles.

Table S6: Band edge potential of various Eu-doped BSO

Material Information	CB(scan 1) (eV)	CB(scan 1) (eV)	CB(scan 1) (eV)	CB (Avg. + SD) (eV)	Bang gap E_g (eV)	VB (eV)
BSO	1.0	-0.98	-0.94	-0.97 ±0.02	3.62	2.65 ±0.02
$Eu_{0.5}$ -BSO	-1.16	-0.97	-0.94	-1.02 ±0.09	3.63	2.61±0.09
$Eu_{1.0}$ -BSO	-1.07	-1.009	-0.96	-1.01± 0.04	3.64	2.63± 0.04
$Eu_{1.5}$ -BSO	-0.63	-0.61	-0.58	-0.61 ±0.02	3.83	3.22±0.02
$Eu_{2.0}$ -BSO	-0.61	-0.608	-0.607	-0.61 ±0.001	3.80	3.19±0.001

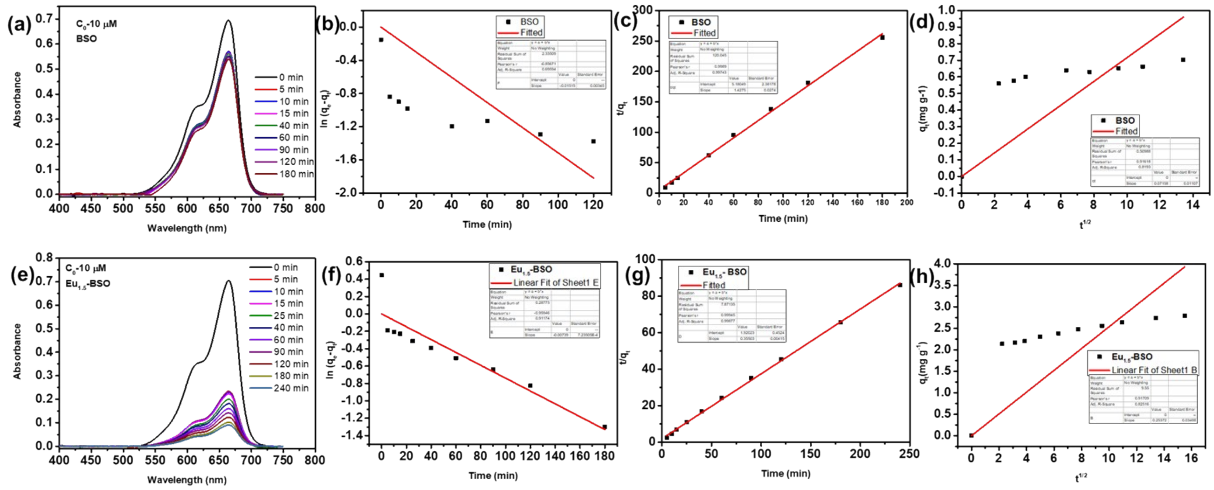

Fig. S14: (a) Absorption spectra for adsorption of MB dye using BSO nanoparticles (b) Fit of kinetic data to pseudo first order model for BSO nanoparticles (c) Fit of kinetic data to pseudo second order model for BSO nanoparticles d) Fit of kinetic data to intraparticle diffusion model for BSO nanoparticles (e) Absorption spectra for adsorption of MB dye using $Eu_{1.5}$-BSO nanoparticles (f) Fit of kinetic data to pseudo first order model for $Eu_{1.5}$-BSO nanoparticles (g) Fit of kinetic data to pseudo second order model for $Eu_{1.5}$-BSO nanoparticles (h) Fit of kinetic data to intraparticle diffusion model for $Eu_{1.5}$-BSO nanoparticles.

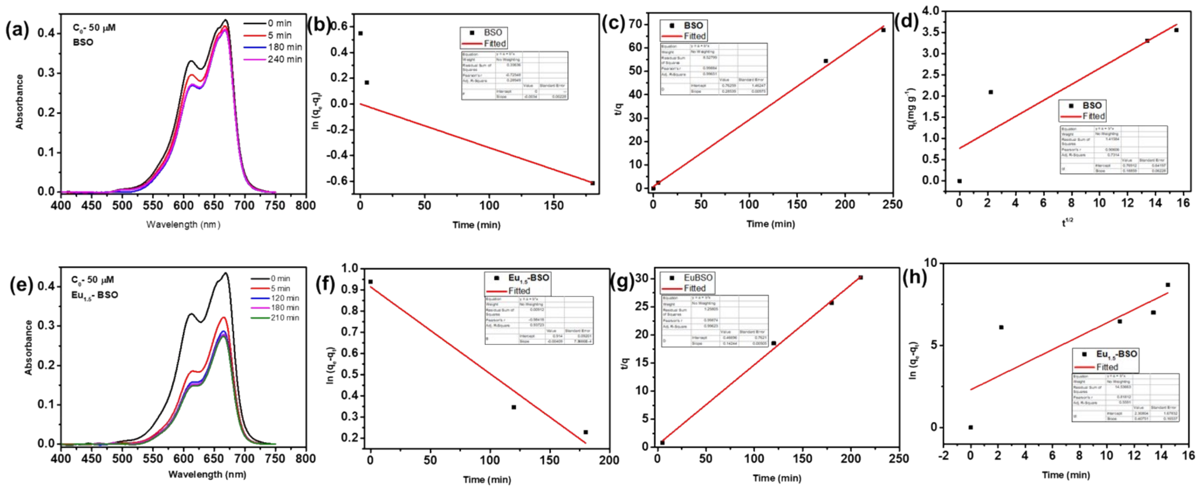

Fig. S15: (a) Absorption spectra for adsorption of MB dye using BSO nanoparticles (b) Fit of kinetic data to pseudo first order model for BSO nanoparticles (c) Fit of kinetic data to pseudo second order model for BSO nanoparticles d) Fit of kinetic data to intraparticle diffusion model for BSO nanoparticles (e) Absorption spectra for adsorption of MB dye using $Eu_{1.5}$-BSO nanoparticles (f) Fit of kinetic data to pseudo first order model for $Eu_{1.5}$-BSO nanoparticles (g) Fit of kinetic data to pseudo second order model for $Eu_{1.5}$-BSO nanoparticles (h) Fit of kinetic data to intraparticle diffusion model for $Eu_{1.5}$-BSO nanoparticles.

Table S7: Kinetics parameters for BSO and $Eu_{1.5}$-BSO nanoparticles for adsorption of methylene blue dye for different initial concentration of dye

		Pseudo first order			Pseudo second order				IPD	
	$q_{e,exp}$ (mg g^{-1})	q_e (mg g^{-1})	k_1 (min^{-1})	R^2	q_e (mg g^{-1})	k_2 (g mg^{-1} min^{-1})	R^2	h ($k_2 q_{e\,exp}{}^2$)	k_1	R^2
BSO (10μM)	0.704	1	$3.5x10^{-2}$	0.69594	0.70052	$39.3x10^{-2}$	0.99743	0.2047	0.07518	0.8193
$Eu_{1.5}$-BSO (10μM)	2.784	1	$1.7x10^{-2}$	0.91174	0.81763	$6.5x10^{-2}$	0.99877	0.5038	0.25730	0.82516
BSO (50μM)	3.552	1	0.0078	0.289	3.49772	$10.7x10^{-2}$	0.99651	1.3499	0.1886	0.7314
$Eu_{1.5}$-BSO (50μM)	8.7	8.2032	0.00941	0.93723	7.02049	$4.3x10^{-2}$	0.99623	3.2546	0.4075	0.5591

Table S8: Comparison table for adsorption of pollutants by various reported materials

Adsorbent	Adsorbate	q_e (mg g^{-1})	Kinetics ($k_1/k_2/k_i$)	Reference
$Eu_{1.5}$-BSO BSO	Methylene blue Methylene blue	8.7 3.5	6.5 *10^{-2} 39.3 *10^{-2}	**This work**
Magnesium Silicate/Reduced Graphene Oxide	Methylene blue	101	3.3 *10^{-3}	[1]
magnetic graphene oxide	Methylene blue	256.4	5.0 *10^{-4}	[2]
Magnesium silicate	Methylene blue	49.8	1.1 *10^{-2}	[3]
Sewage sludge based granular activated carbon (SSGAC)	Methylene blue	27.68	1.6 *10^{-2}	[4]
Moroccan clay	Methylene blue	172.8	5.0 *10^{-3}	[5]
manganese nodule	Methylene blue	51.28	1.9 *10^{-2}	[6]
Polymer networks	Methylene blue	#	2.9×10^{-3}	[7]
Cellulose	Methylene blue	108.11	1.3×10^{-5}	[8]
supramolecular hydrogel	Methylene blue	#	0.9 *10^{-4}	[9]

 # q_e not calculated in the paper.

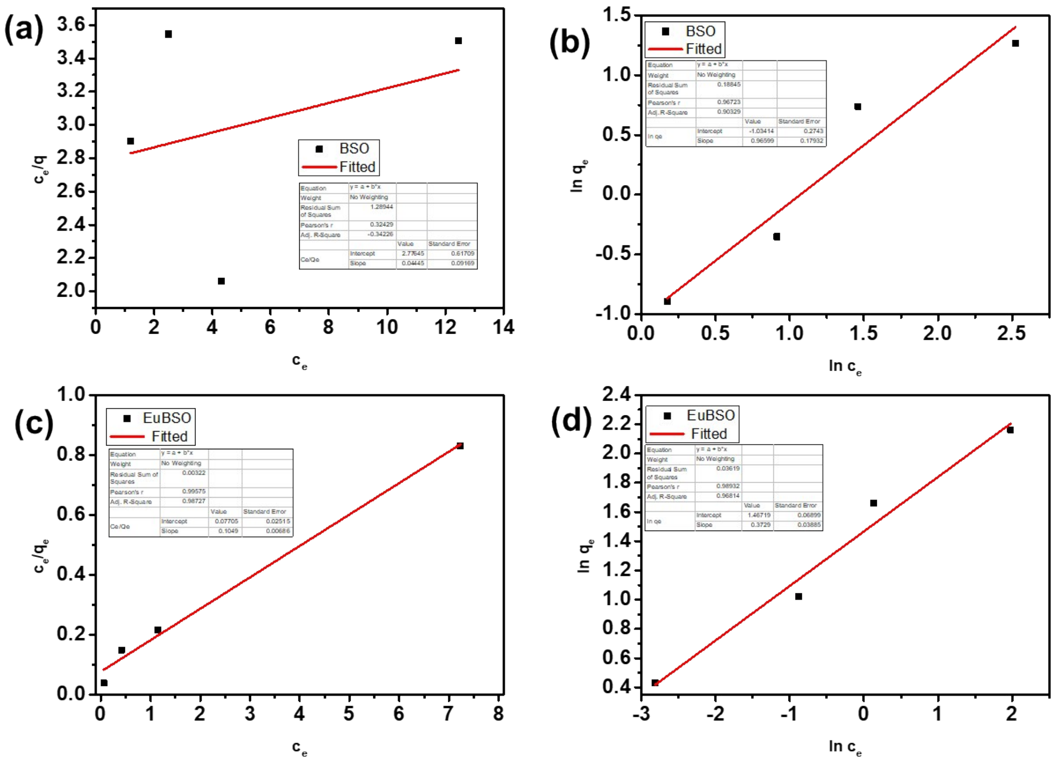

Fig. S16: (a) Langmuir isotherm model fitting for BSO (b) Freundlich isotherm model fitting for BSO nanoparticle (c) Langmuir isotherm model fitting for $Eu_{1.5}$-BSO (b) Freundlich isotherm model fitting for $Eu_{1.5}$-BSO nanoparticle.

Table S9: Comparison table for adsorption isotherm model of methylene blue for BSO and $Eu_{1.5}$-BSO nanoparticle.

		Freundlich			**Langmuir**		
	experimental qmax (mg g^{-1})	k_F	1/n	R^2	qm (mg g^{-1})	b (L mg^{-1})	R^2
BSO	3.552	0.355532	0.96599	0.90329		0.016	-0.34226
$Eu_{1.5}$-BSO	8.7	4.336814	0.3729	0.96814	9.5328	1.3607	0.98727

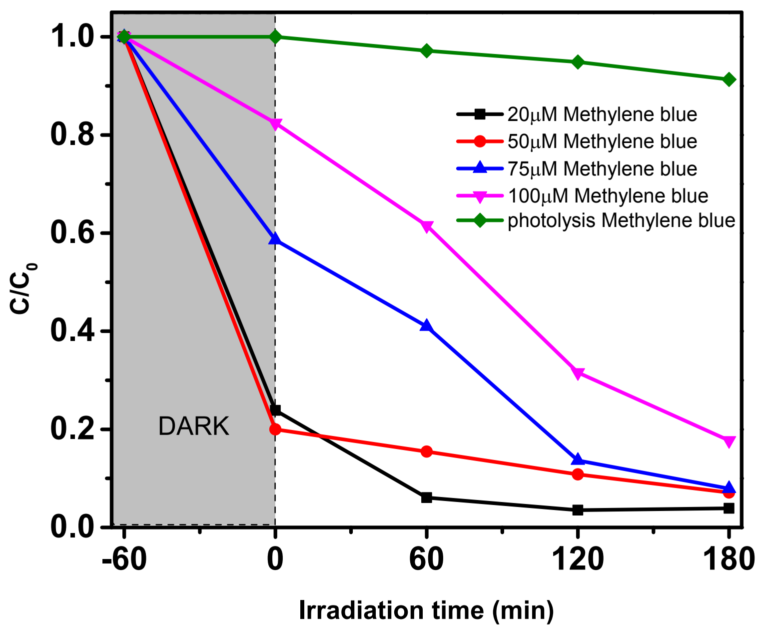

Fig. S17: Photocatalytic degradation of different amount of methylene blue dye by $Eu_{1.5}$-BSO nanoparticles under simulated solar light.

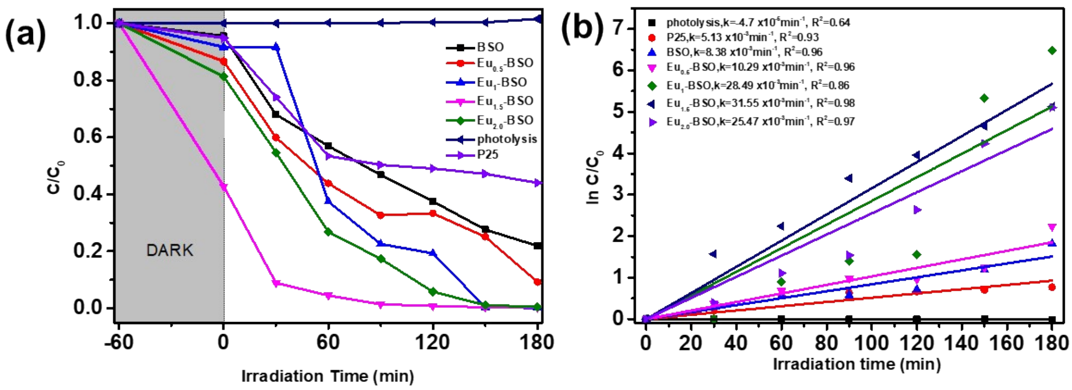

Fig. S18: (a) Photocatalytic degradation of rhodamine B dye (50μM) in presence of BSO and $Eu_{1.5}$-BSO nanoparticles under simulated solar light. (b)Rate of photodegradation of rhodamine B dye calculated assuming first order kinetics.

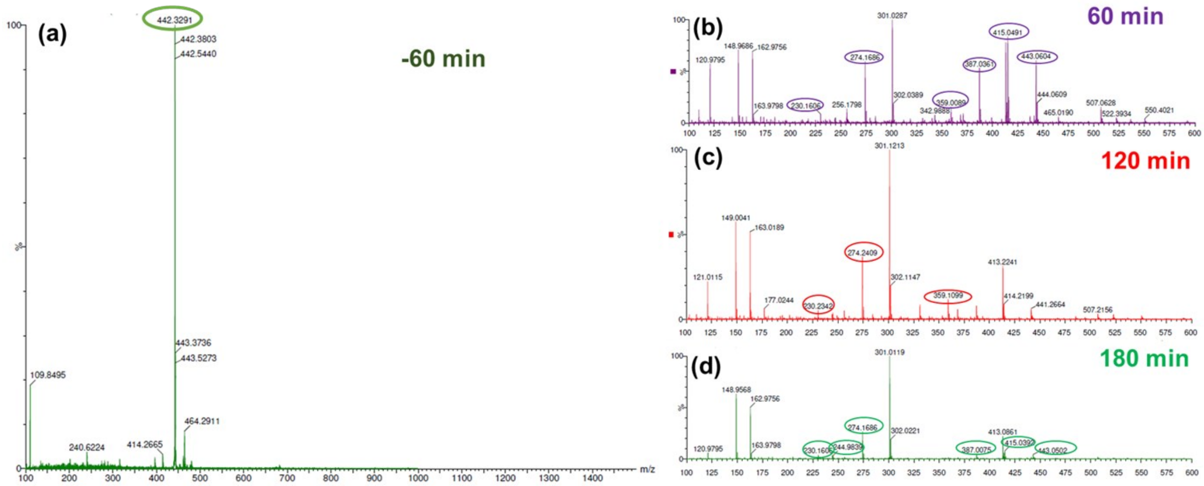

Fig. S19: ESI-MS spectra of aliquots of rhodamine B collected at different points of light illumination. (a) -60 min (represents dye without catalyst) (b) 60 min (c) 120 min (d) 180 min.

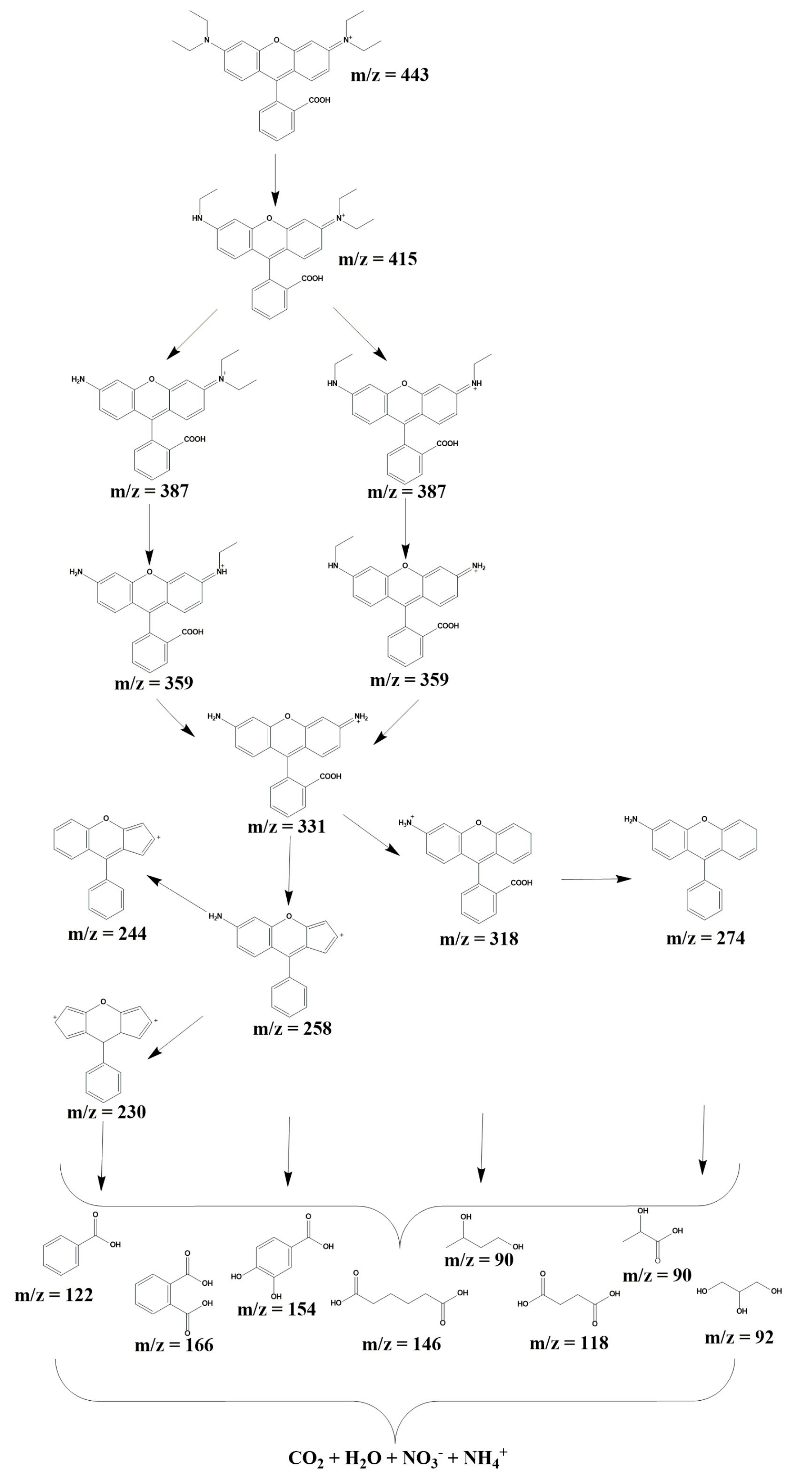

Fig. S20: Possible degradation pathway of rhodamine B

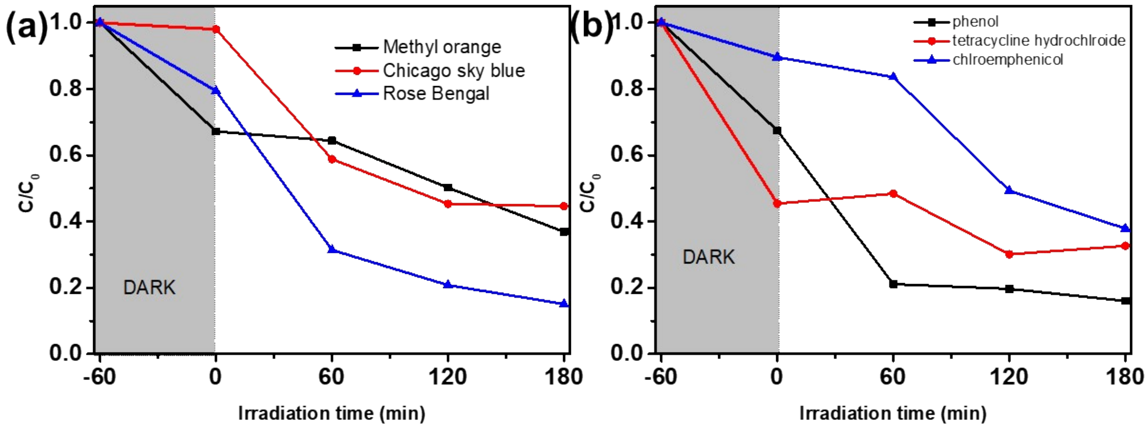

Fig. S21: (a) Photocatalytic degradation of various coloured dyes in presence $Eu_{1.5}$-BSO nanoparticles under simulated solar light. (b) Photocatalytic degradation of various colourless pollutants in presence $Eu_{1.5}$-BSO nanoparticles under simulated solar light.

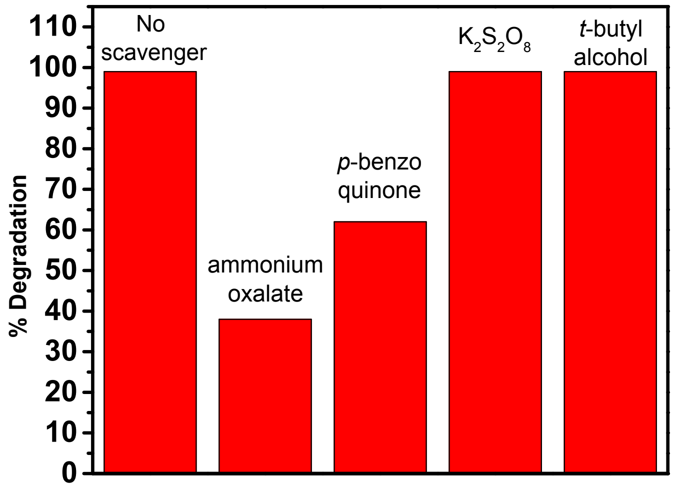

Fig. S22: Radical species trapping experiments for the photocatalytic degradation.

Table S10: Comparison of BET surface area and photocatalytic degradation using Bi_2SiO_5 nanoparticles

Material	BET surface area (m^2/g)	Morphology	Pollutant	Pollutant removal rate	Light Source	Reference
$Eu_{1.5}$-BSO	70	microflower	rhodamine B	99% in 120 min	140 W Xe (simulated solar light) 1.5 AM Filter	**This work**
			methylene blue	98% in 180 min		
			phenol	85% in 180 min		
			methyl orange	62% in 180 min		
			Chicago sky blue	55% in 180 min		
			rose bengal	90% in 180 min		
			tetracycline	70% in 180 min		
			chloremphenicol	70% in 180 min		
Bi_2SiO_5	45	microspheres	phenol	94% in 80 min	500 W Xe (simulated solar light)	10
			rhodamine B	30 % in 30 min		
Bi_2SiO_5/BiOBr	9	nanosheets	rhodamine B	99.5% in 60 min	300 W Xe lamp	11
$Bi_2SiO_5/Bi_{12}SiO_{20}$	33	coralline	acid orange 7	90% in 30 min	100 W Hg lamp	12
			rhodamine B	90% in 30 min		
			p-chlorophenol	90% in 30 min		
			tetracycline	80% in 30 min		
Bi_2O_3/Bi_2SiO_5	66	irregular	Methylene blue,	0.25 h^{-1}	500 W Xe lamp	13
			2,4-Dichlorophenol	0.9 h^{-1}		
			phenol	0.18 h^{-1}		
$Bi_2SiO_5/BiPO_4$	16	plate-like	Methylene blue	9.5 * 10^{-3} min^{-1}	500 W Xe lamp	14
			phenol	9.5 * 10^{-3} min^{-1}		
BiOBr/Bi_2SiO_5	13	irregular nanosheets	tetracycline	90% in 180 min	300 W Xe lamp	15
$Bi_2SiO_5/Bi_4Si_3O_{12}$	1	Flower	Rhodamine	90% in 30 min	300 W Xe Photocatalytic chamber	16
Bi_2SiO_5	30	flower-like microsphere	phenol	86 % in 5h	500 W Xe Lamp (simulated solar light)	17
Bi_2SiO_5	4-6	Nanosheets	salicylic acid	99% in 120 min	4W	18

					UV lamp	
Bi_2O_3/Bi_2SiO_5	8	Irregular	bisphenol A	90% in 120 min	500 W Xe Lamp (simulated solar light)	19
Pt/Bi_2SiO_5	(not provided)	Flower like	7α-ethynylestradiol(EE2)	95.6% in 8 min	20 W Hg UV lamp	20

References

1 C. X. Gui, Q. Q. Wang, S. M. Hao, J. Qu, P. P. Huang, C. Y. Cao, W. G. Song and Z. Z. Yu, *ACS Appl. Mater. Interfaces*, 2014, **6**, 14653–14659.

2 Y. Guo, J. Deng, J. Zhu, X. Zhou and R. Bai, *RSC Adv.*, 2016, **6**, 82523–82536.

3 F. Ferrero, *J. Environ. Sci.*, 2010, **22**, 467–473.

4 L. Liu, Y. Lin, Y. Liu, H. Zhu and Q. He, *J. Chem. Eng. Data*, 2013, **58**, 2248–2253.

5 Y. El Mouzdahir, A. Elmchaouri, R. Mahboub, A. Gil and S. A. Korili, *J. Chem. Eng. Data*, 2007, **52**, 1621–1625.

6 K. M. Parida, S. Sahu, K. H. Reddy and P. C. Sahoo, *J. Chem. Eng. Data* **2007**, 52 , 1621–1625.

7 H. P. C. V. Kuringen, G. M. Eikelboom, I. K. Shishmanova, D. J. Broer and A. P. H. J. Schenning, *Adv. Funct. Mater.*, 2014, **24**, 5045–5051.

8 L. Liu, Z. Y. Gao, X. P. Su, X. Chen, L. Jiang and J. M. Yao, *ACS Sustain. Chem. Eng.*, 2015, **3**, 432–442.

9 B. O. Okesola and D. K. Smith, *Chem. Commun*, 1116, **49**, 11164.

10 L. Dou, J. Zhong, J. Li, J. Luo and Y. Zeng, *Mater. Res. Bull.*, 2019, **116**, 50–58.

11 B. Chai, J. Yan, G. Fan, G. Song and C. Wang, *J. Alloys Compd.*, 2019, **802**, 301–309.

12 W. Q. Li, Z. H. Wen, S. H. Tian, L. J. Shan and Y. Xiong, *Catal. Sci. Technol.*, 2018, **8**, 1051–1061.

13 H. Lu, Q. Hao, T. Chen, L. Zhang, D. Chen, C. Ma, W. Yao and Y. Zhu, *Appl. Catal. B Environ.*, 2018,

237, 59–67.

14 D. Liu, W. Cai, Y. Wang and Y. Zhu, *Appl. Catal. B Environ.*, 2018, **236**, 205–211.

15 J. Wang, G. Zhang, J. Li and K. Wang, *ACS Sustain. Chem. Eng.*, 2018, **6**, 14221–14229.

16 K. Le Jia, J. Qu, S. M. Hao, F. An, Y. Q. Jing and Z. Z. Yu, *J. Colloid Interface Sci.*, 2017, **506**, 255–262.

17 D. Liu, J. Wang, M. Zhang, Y. Liu and Y. Zhu, *Nanoscale*, 2014, **6**, 15222–15227.

18 R. Chen, J. Bi, L. Wu, W. Wang, Z. Li and X. Fu, *Inorg. Chem.*, 2009, **48**, 9072–9076.

19 L. Zhang, W. Wang, S. Sun, D. Jiang and E. Gao, *CrystEngComm*, 2013, **15**, 10043–10048.

20 Y. Chen, S. Wang, J. Liu, Y. Zhang, Y. Long, L. Li, S. Zhang, L. Wang, and F. Jiang, *J. Photoch. Photobio. A,* 2018, **382,** 111920.